Transient Response of an Erodable Heat Flux Gauge using Finite Element Analysis

David R Buttsworth
Faculty of Engineering and Surveying
University of Southern Queensland
Toowoomba, 4350
Australia
phone 07 4631 2614
fax 07 4631 2526
email buttswod@usq.edu.au

April 10, 2002

Abstract

The transient response of an erodable ribbon element heat flux gauge has been assessed using a two-dimensional finite element analysis. Such transient heat flux gauges have previously been used for measurements in internal combustion engines. To identify the heat flux from the measurements of surface temperature, it is commonly assumed that the heat transfer within these devices is one-dimensional. A corollary of the one-dimensional treatment is that only one value of thermal product, $\sqrt{\rho ck}$ is needed for identification of the transient heat flux even though erodable heat flux gauges are constructed from at least two different materials. The current results demonstrate that two-dimensional transient heat conduction effects have a significant influence on the surface temperature measurements made with these devices. For the ribbon element gauge and time scales of interest in IC engine studies, using a one-dimensional analysis (and hence a single value of $\sqrt{\rho ck}$) will lead to substantial inaccuracy in the derived heat flux measurements.

Keywords Transient response, heat flux gauge, erodable thermocouple, engine heat transfer measurements, surface thermometry, instrumentation

1 Introduction

In-cylinder heat transfer has a strong influence on internal combustion (IC) engine performance, efficiency, and emissions. Various electrical resistance and thermocouple devices have been used for instantaneous heat flux measurements in IC engines (see Lawton [1] for a review). Erodable thermocouple heat flux gauges are often used in IC engine work because they are relatively low cost and robust devices with demonstrated delay/rise times typically less than 30μs [2],[3]. Such fast response times are achieved because a low thermal inertia junction is created by sanding or scratching the surface of the gauge; the thermocouple materials themselves form part of the nominally semi-infinte gauge substrate.

Erodable thermocouple heat flux gauges provide a measurement of temperature close to the surface of the gauge because of the low thermal inertia of the junction. To identify the instantaneous heat flux from the measured surface temperature history, it is necessary to apply a suitable model for the transient heat conduction process within the gauge. The usual model is that of one-dimensional heat conduction [1],[2],[4],[5]. Under such conditions, the only parameter that enters the analysis for identification of the transient component of heat flux is the gauge thermal product, $\sqrt{\rho ck}$.

Attempts have been made to identify suitable values of $\sqrt{\rho ck}$ for erodable gauges through calibration [2], although it is sometimes assumed that the thermal properties of the gauge will be dominated by the surrounding material into which the thermocouple is embedded [4]. However, the composite construction

of erodable gauges makes it unlikely a single value of $\sqrt{\rho ck}$ can be applied at all frequencies of interest. As discussed in [3], calibrations to identify $\sqrt{\rho ck}$ should ideally be performed on the time scales of interest in the actual experiments. However, if the one-dimensional heat conduction assumption is fundamentally flawed for the time scales of interest, even such calibrations may not ensure the accurate deduction of heat flux.

In this article, a two-dimensional finite element (FE) model for an erodable heat flux gauge is established. The transient response of this model gauge is investigated in order to investigate the possible limitations of the commonly-applied one-dimensional heat conduction assumption.

2 Gauge Arrangement

The heat flux gauge configuration considered in the present article is illustrated in Fig. 1. It consists of chromel and alumel ribbon elements both 25μm thick that are insulated from each other and the surrounding material (an aluminium alloy, dural in this case) by mica sheets with a thickness of 5μm. Very low thermal inertia k-type thermocouple junctions are created by sanding the surface. In this process, microscopic elements of thermocouple material bridge the central mica insulation, and junctions are made near the surface of the chromel and/or alumel ribbons. This is the ribbon element configuration described by Gatowski et al. [2] with the exception that the surrounding material is an aluminium alloy as used by Oude Nijeweme et al. [4] rather than cast iron.

3 Finite Element Modelling

For simplification of the finite element (FE) model, the chromel and alumel materials were considered as having the same thermal properties. Making this assumption, the y-axis in Fig. 1 is aligned with a plane of symmetry and this enables modelling of only half the actual gauge. Although this assumption is not strictly correct, (the actual differences in ρ, c, and k are around 30% [6],[3]), it is reasonable since there are large uncertainties in the thermal properties (in particular, the thermal conductivity) of mica. Given the above uncertainties and simplifications, round-figure estimates for the thermal diffusivity α and thermal product $\sqrt{\rho ck}$ of each material were adopted as presented in Table 1.

A finite element package, ANSYS 5.7 was used for this work. Any set of ρ, c, and k values giving the desired values of α and $\sqrt{\rho ck}$ could have been chosen for use with the software. Densities close to the physically correct values were chosen for each material, and values of c and k consistent with the adopted values of α and $\sqrt{\rho ck}$ were derived (Table 1).

The FE model extended a distance of 0.2mm in the x-direction and 1mm in the y-direction. Elements with mid-side nodes were used. At the exposed surface of the gauge (y=0), the element length in the y-direction was 0.5μm. Element lengths in the y-direction increased with distance from the surface. At the exposed surface of the gauge (y=0), the element length in the x-direction was 0.5μm within the mica sheets. The surface of the thermocouple material was discretised using elements with an average x-length of 1.25μm with compression towards the mica material at either edge of the ribbon.

The grit size of the abrasive paper used to create the junctions will affect the thickness of the bridging material, and hence the response of the gauge. However, for typical gauge constructions, delay/rise times of less than 30μs have been observed [2], [3]. Hence, it was not necessary to model the thermocouple material that bridges the mica insulation, as the time scales of primary interest in the present work are on the order of milliseconds.

The accuracy of the FE modelling was assessed by considering a dural sheet with identical dimensions and meshing to the mica sheet running along the x=0 boundary in the full model. A heat flux step of 1MW/m^2 was applied at the exposed surface of this dural sheet, and the remaining surfaces of the model had zero heat flux boundary conditions. A solution was obtained using a constant time step size of 2.5μs up to a maximum time of 10ms. Figure 2 presents the surface temperature history produced by FE modelling normalised using the semi-infinite one-dimensional solution. That is, the surface temperature from the FE solution relative to the initial temperature of the material, $T - T_i$ has been divided by the semi-infinite one-dimensional solution,

$$(T - T_i)_{si-1d} = \frac{2q\sqrt{t}}{\sqrt{\pi}\sqrt{\rho ck}} \tag{1}$$

Following the step in surface heat flux (at t=0), a finite time is required for the FE solution to approach the correct solution, $(T - T_i)/(T - T_i)_{si-1d} = 1$, as indicated in Fig. 2. For the dural material and a time step size of 2.5μs, approximately 30μs were required for the surface temperature to approach with 1% of the true solution. The FE solution remains within 1% of the semi-infinite one-dimensional solution up to 6.4ms. The departure of the FE solution after approximately 6.4ms (see Fig. 2) is due to the zero heat flux boundary condition at y=1mm (the maximum extent of the model) which results in a more rapid rise of surface temperature than would occur in a semi-infinite one-dimensional situation.

4 Gauge Response to Heat Flux Step

A step in heat flux was applied at the surface of the full FE model of the gauge. Selected temperature histories and distributions from this analysis are presented in Fig. 3. The surface temperature of the

mica and thermocouple materials rises faster than that of the dural because of the lower values of $\sqrt{\rho ck}$ for the mica and thermocouple materials (see Table 1). The surface temperature of the dural rises faster than the semi-infinite one-dimensional result (the broken line in Fig. 3a) because: 1) the model has a finite extent in the y direction (as discussed in Section 3); and 2) heat is conducted laterally into the dural from the mical sheet (and thermocouple ribbon).

The position of the effective junction location on the thermocouple material is probably affected by the abrasive paper grit size used to create the junction. While the junction location will influence the gauge response, Fig. 3 indicates that the surface temperature is reasonably uniform across the entire surface of the ribbon element. The centre of the ribbon has been chosen as a representative thermocouple junction location.

Figure 4 presents the surface temperature history at the centre of the thermocouple ribbon normalised using the semi-infinite one-dimensional solution with the value of $\sqrt{\rho ck}$ taken as that of the dural. For the results in Fig. 4, an initial time step size of 5ns was taken. This resulted in the FE solution approaching within 1% of the semi-infinite one-dimensional solution, $(T-T_i)/(T-T_i)_{si-1d} = 2$ at t=60ns. The factor of 2 arises because the assumed thermal product of the dural material is twice that of the thermocouple material (Table 1).

The gauge behaves in a semi-infinite one-dimensional manner for only a short time (around 2μs - see Fig. 4a) before the surface temperature increases more rapidly due to the additional heat conduction into the thermocouple ribbon from the mica material. This causes the normalised surface temperature at the thermocouple ribbon surface to rise to a peak value of $(T-T_i)/(T-T_i)_{si-1d} = 2.239$ at $t = 81\mu$s, Fig. 3a. After this time, the normalised surface temperature begins to fall due to lateral conduction of heat away from the thermocouple and mica materials and into the surrounding dural material, Fig. 3b. However, Fig. 3b indicates that even at t=10ms, the thermocouple surface temperature remains more than 40% higher than the anticipated value for dural material (if semi-infinite one-dimensional conditions applied). The model's finite extent in the y-direction contributes less than about 5% to this difference at t=10ms (see Fig. 2).

5 Gauge Response to Model Heat Flux Variations

Due to the linearity of the governing transient heat conduction equations, the heat flux gauge can be considered as a linear system. In the present context, the output of the system is the surface temperature at the centre of the thermocouple ribbon, and the input to the system is the surface heat flux which is assumed to be uniform across the entire surface of the gauge. The system impulse response was identified

by differentiating the temperature history obtained from the FE model with a step heat flux input.

The thermocouple surface temperature history associated with any particular heat flux history can therefore be simulated through the convolution of the applied heat flux input and the impulse response of the system. To assess the implications of the usual one-dimensional heat conduction assumption, the apparent surface heat flux can then be identified from the simulated surface temperature history using,

$$q(t) = \frac{\sqrt{\rho c k}}{\sqrt{\pi}} \int_0^t \frac{dT}{d\tau} \frac{1}{\sqrt{t-\tau}} d\tau \tag{2}$$

Schultz and Jones [7], and compared with the actual heat flux input at the surface of the gauge. The value of $\sqrt{\rho c k}$ used in Eq. (2) was taken as that of the dural material (Table 1).

The analysis described above has been executed for two model surface heat flux histories. The first model history is a square heat flux pulse of width 2ms ("actual (a)" in Fig. 5) and the second is a sinusoidal heat flux variation with a period of 10ms ("actual (b)" in Fig. 5).

For the square heat flux pulse, the apparent heat flux initially exceeds the actual heat flux by more than a factor of 2 because the initial transient conduction process is dominated by the thermocouple and mica materials, rather than the surrounding dural material. The lateral conduction effects responsible for the observed form of the apparent heat flux have already been discussed in Section 4. An important consequence of the lateral conduction is the negative overshoot that occurs at trailing edge of the pulse. In the present case the apparent heat flux drops to around -0.68MW/m^2 or about -30% of the apparent peak value.

The intention of the sinusoidal variation of actual heat flux ("actual (b)" in Fig. 5) was to provide a variation somewhat representative of the heat flux pulses observed in IC engine experiments. The apparent heat flux still deviates substantially from the actual heat flux for the sinusoidal case. The peak heat flux is more than 50% higher than the actual heat flux because the thermal properties of the embedded ribbon (and mica) differ from those of the surrounding dural material. A negative overshoot in heat flux also occurs for the sinusoidal variation, although it is less significant than for the square pulse. However, by 10ms the finite extent of the FE model in the y-direction influences the results, tending to reduce the magnitude of the apparent heat flux overshoot relative to the value that would be obtained with a more extensive FE model.

6 Conclusions

There are certain limitations of the present modelling including non-semi-infinite boundary conditions, and material properties uncertainties (particularly for the insulating material). Furthermore, only one special type of erodable thermocouple - a ribbon element configuration - has been considered. However, the intention of this article is not to provide exhaustive results applicable to all erodable gauge configuration. The primary intention of this article is to alert workers to possible errors arising from the accepted one-dimensional modelling of similar erodable thermocouple constructions.

For the time scales of interest in IC engine experiments, it is incorrect to assume that the response of the gauge is governed by the thermal properties of the surrounding material. The thermal properties of the surrounding material do have an impact, but the properties of the thermocouple and insulation materials also make an important contribution to the net response.

A one-dimensional treatment of the transient surface temperature data produced using this type of erodable thermocouple appears inappropriate for the time scales of interest in IC engine experiments. Significant lateral conduction occurs for events with time scales between about 1ms and 10ms (or more). This lateral conduction can result in an apparent (negative) overshoot in response when the level of heating is reduced (if the analysis assumes one-dimensional behaviour). Such a situation arises during the expansion stroke of an IC engine and negative heat flux values have been registered for both motored [5] and fired [4] engines even when the gas temperature remains higher than the surface temperature. Negative heat flux results have previously been explained using unsteady boundary layer models [5],[4]. However, the present results suggest that some portion of the negative heat flux may actually be an artefact from the one-dimensional transient heat conduction modelling.

If erodable thermocouples are to be used for transient heat flux measurements, the transient response of the gauge should be confirmed for the time scales of interest using a finite element analysis along the lines described in this article, and/or a suitable calibration technique [2],[3]. If the transient conduction within the gauge cannot be accurately treated in a one-dimensional manner, a two-dimensional analysis may be possible with the aid of finite element or finite difference modelling. However, it may prove easier to either redesign the thermocouple instrumentation or perhaps use a different approach that results in one-dimensional transient heat conduction. One such approach involves thin film resistance gauges on a plastic substrate for the measurement of both steady and transient components of the heat flux [8], and this technique has recently been demonstrated in an IC engine [9].

Notation

c	specific heat (J/kgK)
k	thermal conductivity (W/mK)
q	surface heat flux (W/m^2)
t	time, arbitrary or relative to the start of heating (s)
T	temperature at the surface of the gauge (K)
T_i	initial temperature of the gauge (K)
x	lateral distance from the centre of the gauge (m)
y	distance (depth) from surface of gauge (m)
α	thermal diffusivity, $k/\rho c$ (m^2/s)
ρ	density (kg/m^3)
τ	dummy variable for integration wrt time (s)
subscript	
$si-1d$	semi-infinite, one-dimensional solution

References

[1] B. Lawton and G. Klingenberg, *Transient Temperature in Engineering and Science*, Oxford University Press, Oxford, 1996.

[2] J. A. Gatowski, M. K. Smith, and A. C. Alkidas, "An experimental investigation of surface thermometry and heat flux", *Exp. Therm. Fluid Sci.*, vol. 2, pp. 280–292, 1989.

[3] D. R. Buttsworth, "Assessment of effective thermal product of surface junction thermocouples on millisecond and microsecond time scales", *Experimental Thermal and Fluid Science*, vol. 25, no. 6, pp. 409–420, 2001.

[4] D. J. Oude Nijeweme, J. B. W. Kok, C. R. Stone, and L. Wyszynski, "Unsteady in-cylinder heat transfer in a spark ignition engine: experiments and modelling", *Proc. IMechE - Part D: J. Automobile Eng.*, vol. 215, pp. 747–760, 2001.

[5] B. Lawton, "Effect of compression and expansion on instantaneous heat transfer in reciprocating internal combustion engines", *Proc. IMechE - Part A: Power and Process Eng.*, vol. 201, no. A3, pp. 175–186, 1987.

[6] F. R. Caldwell, "Thermocouple materials", in *Applied methods and instruments*, C. M. Herzfeld, Ed., vol. 3 of *Temperature: Its measurement and control in science and industry*, pp. 81–134. Reinhold, New York, 1962.

[7] D. L. Schultz and T. V. Jones, "Heat-transfer measurements in short-duration hypersonic facilities", AGARDograph 165, Advisory Group for Aerospace Research and Development, 1973.

[8] E. Piccini, S. M. Guo, and T. V. Jones, "The development of a new direct-heat-flux gauge for heat transfer facilities", *Meas. Sci. Technol.*, vol. 11, pp. 342–349, 2000.

[9] T. S. Wilson, P. Bryanston-Cross, K. S. Chana, P. Dunkley, T. V. Jones, and P. Hannah, "High bandwidth heat transfer and optical measurements in an instrumented spark ignition internal combustion engine", 2002, SAE Paper 2002-01-0747.

	mica	thermocouple	dural
α (m^2/s)	10×10^{-6}	5×10^{-6}	50×10^{-6}
$\sqrt{\rho ck}$ ($J/m^2Ks^{1/2}$)	0.5×10^{3}	10×10^{3}	20×10^{3}
ρ (kg/m^3)	2800	8600	2800
c (J/kgK)	56.47	520.0	1010
k (W/mK)	1.581	22.36	141.4

Table 1: Assumed thermal properties of the mica, thermocouple, and dural materials.

List of Figures

1 Illustration of the erodable ribbon element thermocouple configuration. 12

2 Normalised surface temperature from FE analysis for assessment of accuracy. 13

3 Surface temperature results for the gauge. 14

4 Normalised surface temperature history at the centre of thermocouple ribbon. 15

5 Illustration of errors introduced by one-dimensional treatment for: a) square heat flux pulse of width 2ms; and b) sinusoidal heat flux variation with a 10ms period as illustrated. 16

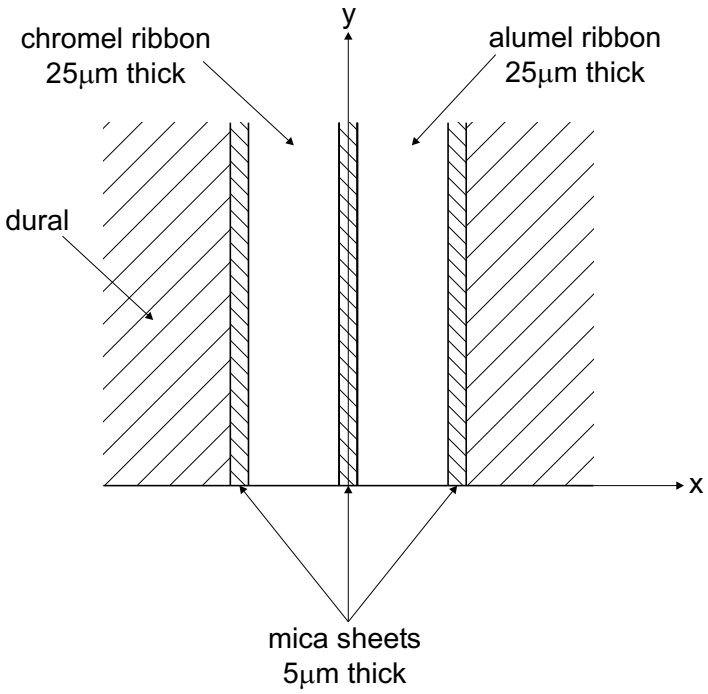

Figure 1: Illustration of the erodable ribbon element thermocouple configuration.

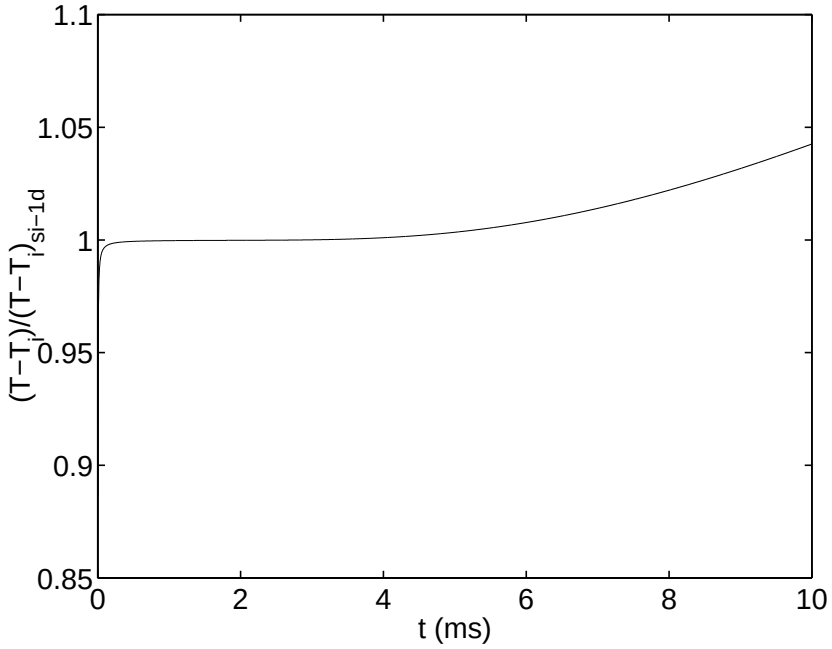

Figure 2: Normalised surface temperature from FE analysis for assessment of accuracy.

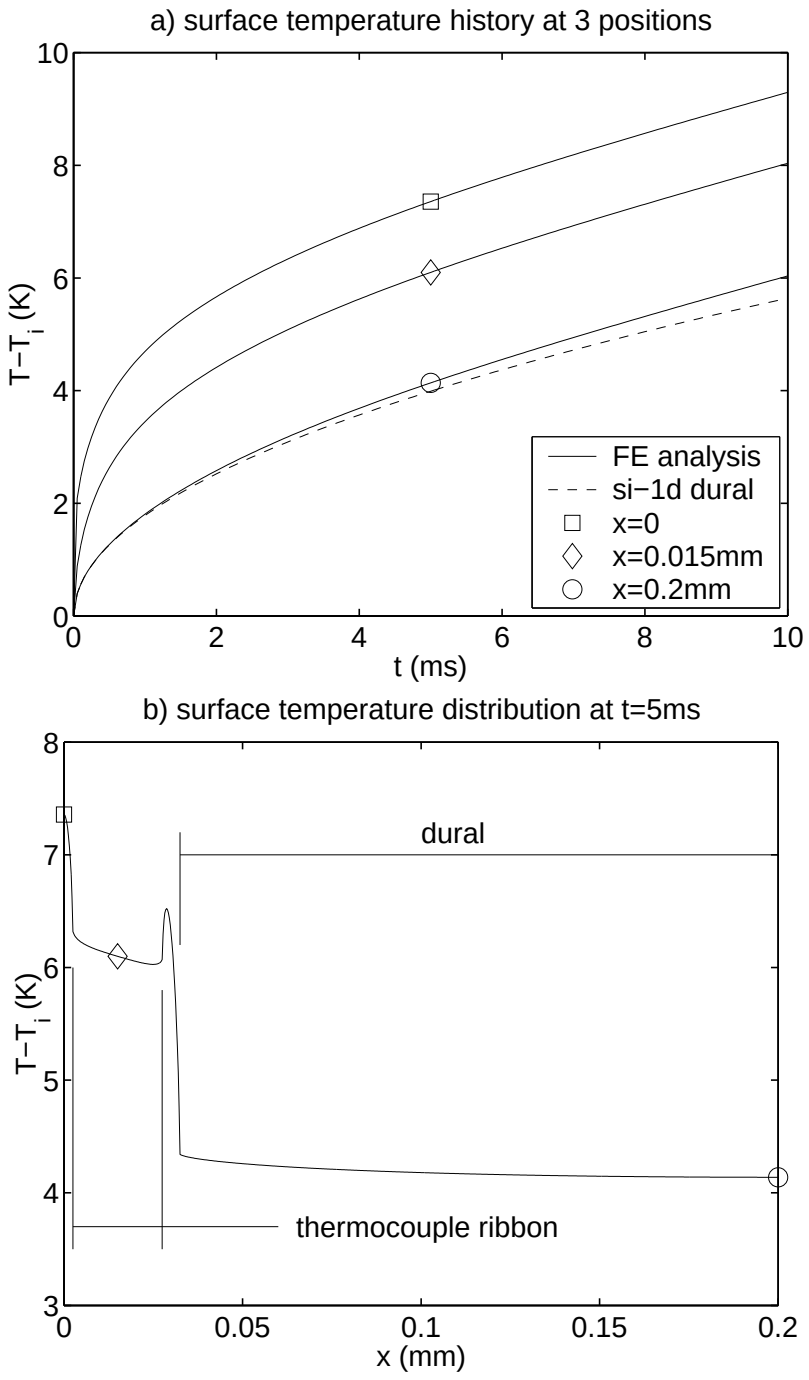

Figure 3: Surface temperature results for the gauge.

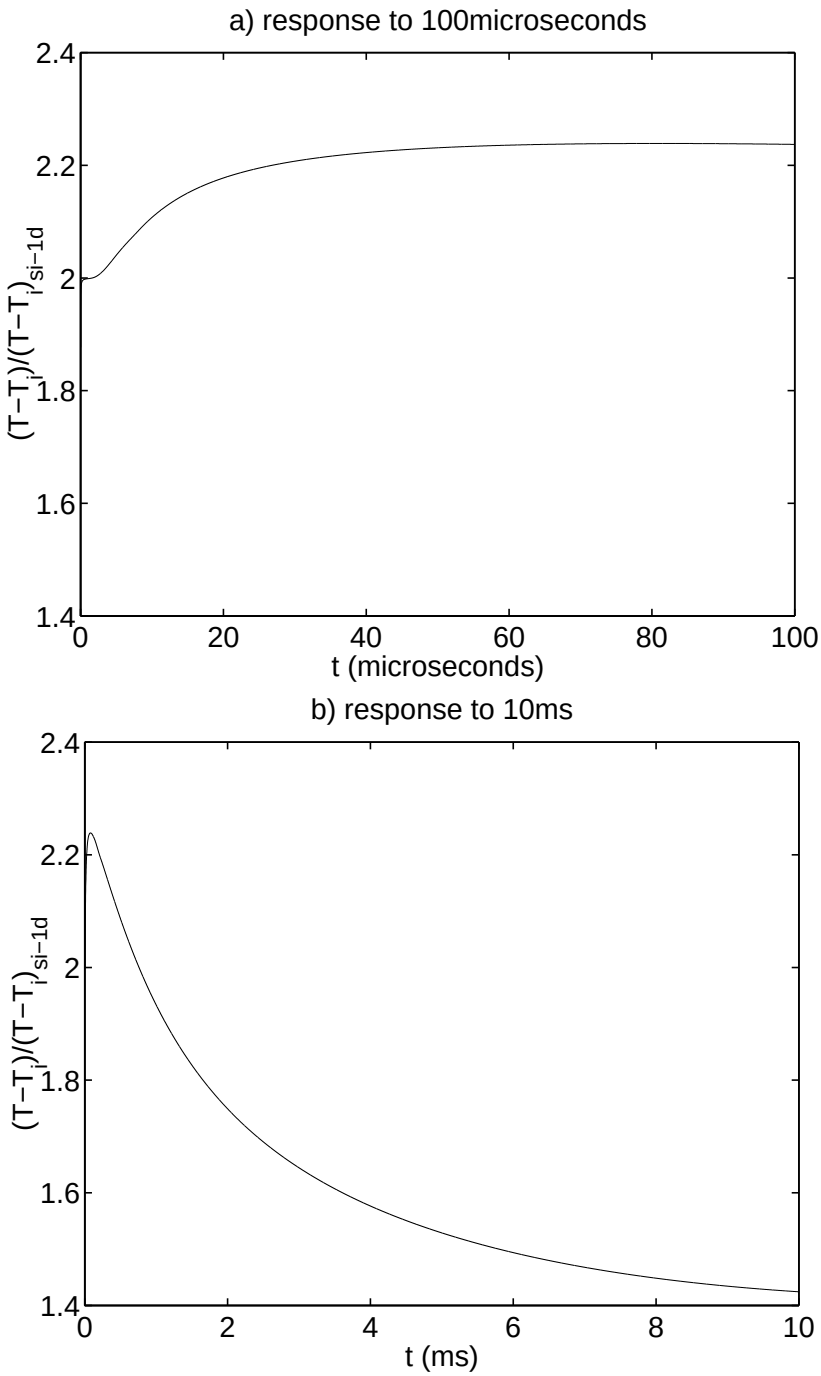

Figure 4: Normalised surface temperature history at the centre of thermocouple ribbon.

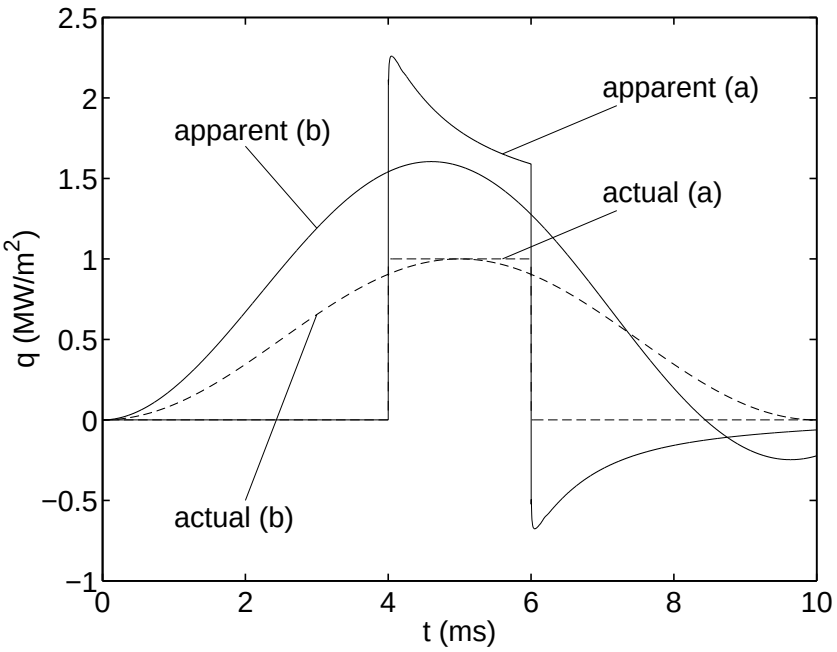

Figure 5: Illustration of errors introduced by one-dimensional treatment for: a) square heat flux pulse of width 2ms; and b) sinusoidal heat flux variation with a 10ms period as illustrated.